Fermilab Library
0 1160 0031769 7

u c s b High Energy Physics

UCSB-HEP-93-06
Sept 1993

23

CHARM DECAY PHYSICS*

MICHAEL S. WITHERELL
Department of Physics
University of California
Santa Barbara, California, 93106-9530

FERMILAB
LIBRARY
OCT 18 1993

ABSTRACT

I review the experimental results on the weak decays of charm particles, and the related physics issues.

Invited talk given at the International Symposium on Lepton and Photon Interactions at High Energies, Cornell University, Ithaca, NY (August 1993).

* Supported by the U.S. Department of Energy Award No. DE-FG03-91-ER40618

Charm Decay Physics

M.S.Witherell

Dept. of Physics, University of California, Santa Barbara

(September 29, 1993)

I review the experimental results on the weak decays of charm particles, and the related physics issues.

I. INTRODUCTION

It is 17 years since the discovery of the decays $D^0 \to K^-\pi^+$ and $D^+ \to K^-\pi^+\pi^+$ at SPEAR (1). The observation of these decays (a) confirmed that the c quark satisfied the predictions of the Glashow, Iliopolous, Maiani mechanism (2); (b) measured the mass of the D mesons; and (c) began the experimental study of weak decays of charm. Since that time a large body of detailed information about charm decays has been collected. These charm decay measurements have come from three different accelerator environments: e^+e^- colliders at threshold (SPEAR, BEPC); e^+e^- colliders in the Υ region (CESR, DORIS); and external beams at proton machines (FNAL, SPS).

Once the nature of the GIM mechanism was established, much of the effort to understand the weak interactions of quarks and the Cabibbo-Kobayashi-Maskawa matrix naturally turned to the study of b quark decays. The question for charm became, "What more can one learn from charm decays?" The answer is not precise CKM parameters, since V_{cs} and V_{cd} are determined from three-generation unitarity better than can be measured directly. Nor is the answer CP phenomenology in the Standard Model, since it is expected to be at a level too small to be measured.

The study of charm decays is pointed toward (a) the search for anomalous weak interactions, such as large mixing or CP violation; (b) the understanding of the nonperturbative strong interactions that are inevitably involved in weak decays of quarks; and (c) the measurement of branching ratios needed for B physics. The second item represents an area of physics in which there has been a large amount of theoretical effort in the last few years. The comparisons between D and B decays reveal the size of effects resulting from the heavy quark being not all that heavy.

I will first introduce the decay diagrams which we use to describe charm decay, using the Cabibbo-allowed decays to illustrate them. Figures 1(a-c) show the spectator decays, in which the light antiquark in the charm meson does not participate in the weak interaction. In the semileptonic decay(a), the charm quark decays to a strange quark, plus a virtual W^+ which decays

© 1993 American Institute of Physics

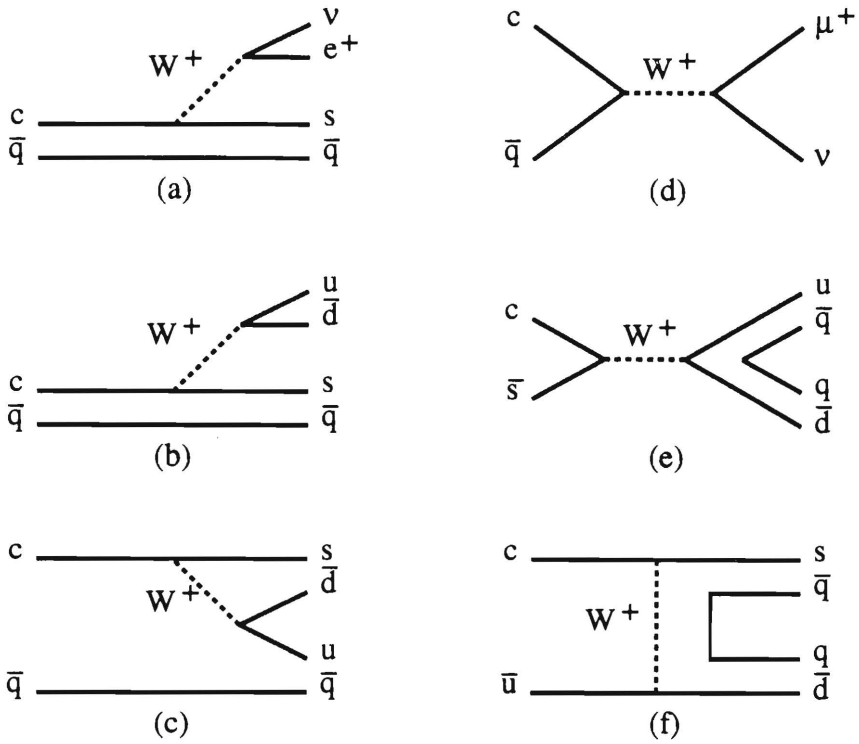

FIG. 1. The diagrams for charm meson decay: (a) semileptonic decay; (b) hadronic spectator decay, type a1; (c) hadronic spectator decay, type a2; (d) leptonic decay; (e) W annihilation decay; (f) W exchange decay.

into $\ell^+\nu$. Form factors describe how the final state $s\overline{q}$ turns into a strange meson.

There are two hadronic spectator diagrams in figure 1. The first one (b) is the direct analog of semileptonic decay, except that the virtual W decays into $u\overline{d}$. I will call this an a_1 diagram, reflecting the fact that in the scheme of Bauer, Stech, and Wirbel (BSW) (3), the semileptonic decay amplitude is multiplied by a factor a_1. The second diagram (c) is sometimes called an internal W diagram, or a color-suppressed diagram; I will call it an a_2 diagram. In it, the $\overline{d}$ antiquark from the weak vertex combines with the strange quark rather than with the spectator quark. It is well known that for D^0 decays, these two diagrams lead to different final states, such as $K^-\pi^+$ and $\overline{K}^0\pi^0$, while for D^+ decays, they both can produce the $\overline{K}^0\pi^+$. The two diagrams interfere destructively for the D^+, increasing its lifetime. In

TABLE 1. Lifetime measurements for D mesons (psec)

Exp.	D^+	D^0	D_s^+
E-687 (4)	$1.048 \pm 0.015 \pm 0.011$	$0.413 \pm 0.004 \pm 0.003$	$0.475 \pm 0.020 \pm 0.007$
E-691 (5)	$1.090 \pm 0.030 \pm 0.025$	$0.422 \pm 0.008 \pm 0.010$	$0.47 \pm 0.04 \pm 0.02$
Ave	1.056 ± 0.017	0.414 ± 0.005	0.474 ± 0.019

the simplest picture of the hadronic decays, one assumes factorization of the decay amplitude, using a decay constant to describe the amplitude for the $u\bar{d}$ ($s\bar{d}$) in the $a_1(a_2)$ diagram to become a given meson.

There are also nonspectator diagrams which can contribute to charm decay, and they are shown in figures 1(d-f). The first is the leptonic decay(d), illustrated by $D_s^+ \to \mu^+\nu_\mu$. There is a helicity suppression for a pseudoscalar meson decaying in this way, as for charged pion decay. The decay rate is proportional to $f_{D_S}^2 m_\ell^2$. This leads to a fairly small muonic branching fraction and a negligible electronic fraction.

The two hadronic nonspectator decays are shown next. The first is the W annihilation diagram(e), such as $D_s^+ \to \rho^0\pi^+$. The other is the W exchange diagram(f), which can contribute to decays such as $D^0 \to \overline{K}^0\pi^0$. Strong interactions mitigate the helicity suppression somewhat, compared to the leptonic decay, but the rate for these decays is still smaller than that for the spectator decays. For decays of charm baryons, there is no helicity suppression, and the W exchange diagram has an amplitude comparable to that for the spectator decay.

II. LIFETIMES

The pattern of charm meson lifetimes can be explained using a simple picture of quark diagrams and factorization, based on two principles: two-body spectator decays dominate, and the two spectator diagrams interfere destructively if the spectator antiquark is the same flavor as the produced antiquark. As I said above, the Cabibbo-allowed D^+ decays have this interference, which causes the lifetime pattern $\tau(D^+) > \tau(D^0) \approx \tau(D_s^+)$. Because $a_2/a_1 \approx -0.4$, $\Gamma_{had}(D^0)/\Gamma_{had}(D^+) \approx 3$, leading to the lifetime ratio $\tau(D^+)/\tau(D^0) \approx 2.5$.

The measurements of D meson lifetimes are now dominated by the analysis of the full data set from the Fermilab photoproduction experiment E-687 (4). The vertex separation cuts using the silicon vertex detector make it possible to achieve very clean, large charm samples. There are 9200 $D^+ \to K^-\pi^+\pi^+$ decays in the sample, for example, with a signal to background ratio(S/B) of about 15 at the peak of the mass spectrum. Because of the tiny statistical error, they studied the systematic errors in detail to obtain a measurement with a total error of about 1.5%. Table 1 is a summary of the lifetime measurements of the D mesons.

The errors from the E-687 lifetime measurements are about a factor of two

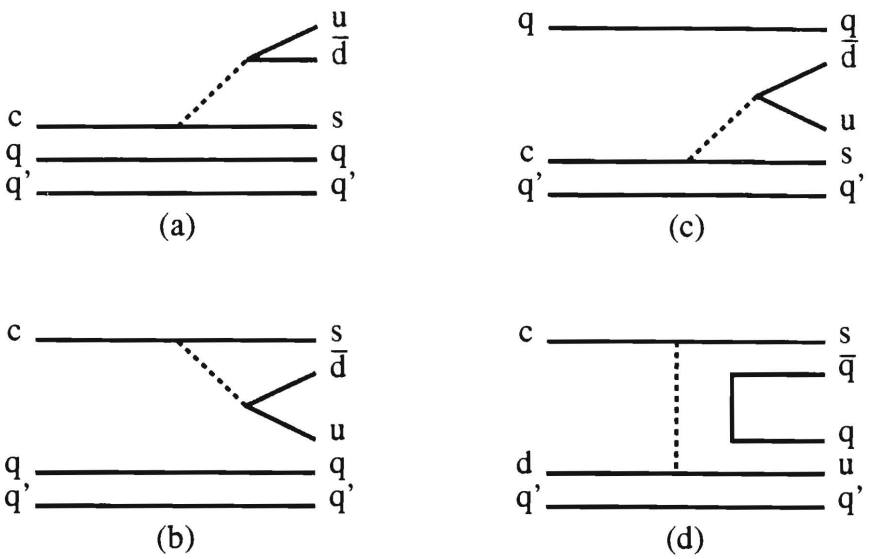

FIG. 2. The diagrams for charm baryon hadronic decay: (a)-(c) hadronic spectator decays; (d) W exchange decay.

better than that of the E-691 data taken in 1985. Together, they dominate the world average. The precision of the lifetime measurements is beyond the ability to calculate them, but precise lifetime ratios are important, especially when comparing decay rates of the different charm mesons. Using the average lifetimes, the ratios are $\frac{\tau(D^+)}{\tau(D^0)} = 2.55 \pm 0.05$ and $\frac{\tau(D_s^+)}{\tau(D^0)} = 1.14 \pm 0.05$.

The pattern of charm baryon lifetimes is more complex than that for the mesons. Four diagrams contribute substantially to the rates, as shown in figure 2. There are three effects which can change the lifetime substantially compared to the bare spectator lifetime seen for the D^0 and D_s^+. [1] As for mesons, there is a destructive interference between diagrams (a) and (c) if a spectator quark is a u quark (Λ_c^+, Ξ_c^+). [2] In addition, there is a constructive interference between diagrams (b) and (c) if a spectator quark is an s quark (Ξ_c^+, Ξ_c^0). [3] Finally, the exchange diagram is not helicity suppressed, and is large if there is a d quark in the charm baryon (Λ_c^+, Ξ_c^0). The relative size of these effects leads to predictions on the pattern of lifetimes. Guberina et al. (6) predict $\tau(\Omega_c) \approx \tau(\Xi_c^0) < \tau(\Lambda_c) < \tau(\Xi_c^+)$, while Voloshin and Shifman (7) predict $\tau(\Omega_c) < \tau(\Xi_c^0) < \tau(\Lambda_c) \approx \tau(\Xi_c^+)$.

Again the full data sample from E-687 provides the most precise information (8). Figure 3(a) shows the $\Lambda_c \to pK^-\pi^+$ sample, with about 700 events and S/B = 1 at the peak. Figure 3(c) shows the lifetime spectrum, with exponential behavior over a few lifetimes. Even for the charmed strange baryons,

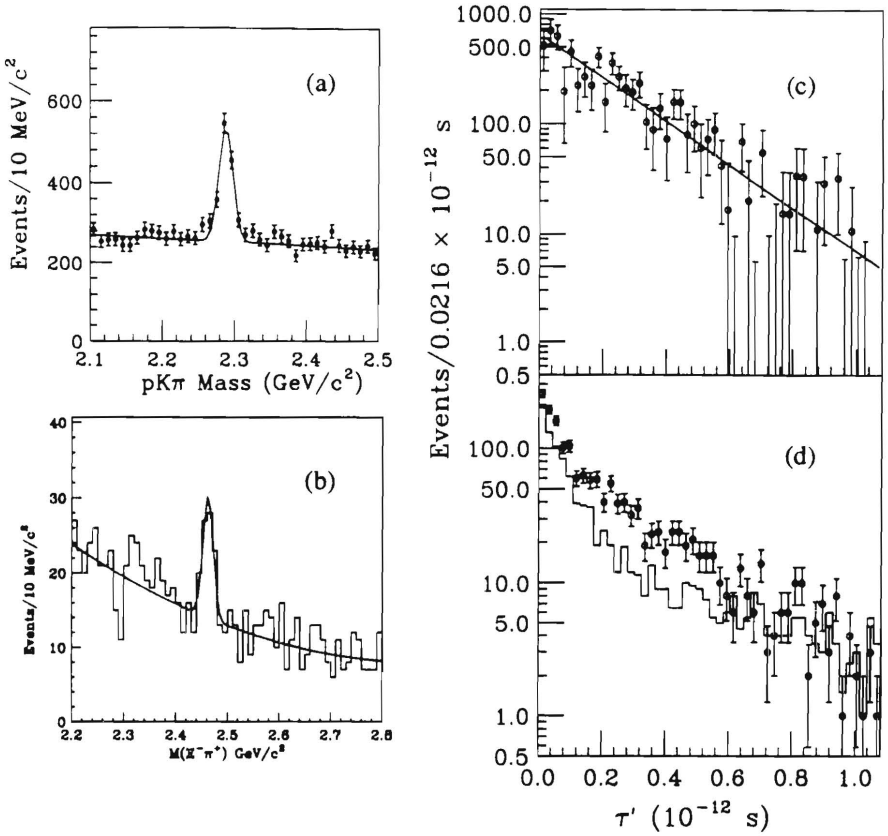

FIG. 3. Charmed baryon data from E-687: (a)Λ_c^+ signal; (b)Ξ_c^0 signal; (c) fit to decay time spectrum for Λ_c^+, after sideband subtraction and efficiency correction; and (d)decay time spectrum for signal(circles) and sideband(histogram) regions.

E-687 obtains clean samples of reasonable size, as shown in Figure 3(b). The lifetime measurements for the baryons are shown in table 2. The E-687 results dominate, although older experiments still contribute significantly to the average. The Λ_c^+ lifetime is about a factor of two less than the D^0. The $\Xi_c^+(\Xi_c^0)$ lifetime is a factor of two greater(less) than $\tau(\Lambda_c^+)$.

As I said earlier, there are three effects that can change the lifetime of a charmed baryon from the bare spectator lifetimes of the D^0. Ignoring differences in masses, etc., one can estimate the sizes of these effects from the three lifetimes in table 2:

$$\Gamma(\Lambda_c^+) = \Gamma(spec) - \Gamma(int-) + \Gamma(exc)$$
$$\Gamma(\Xi_c^0) = \Gamma(spec) + \Gamma(int+) + \Gamma(exc)$$
$$\Gamma(\Xi_c^+) = \Gamma(spec) - \Gamma(int-) + \Gamma(int+) \quad .$$

One sees that the exchange diagram in baryons has an amplitude larger than

TABLE 2. Lifetime measurements for charm baryons (psec)

Exp.	Λ_c^+	Ξ_c^+	Ξ_c^0
E-687 (8)	$0.215 \pm 0.015 \pm 0.008$	$0.41\ ^{+0.11}_{-0.08} \pm 0.02$	$0.101\ ^{+0.025}_{-0.017} \pm 0.005$
NA-32 (9)	$0.196\ ^{+0.023}_{-0.020}$	$0.20\ ^{+0.11}_{-0.06}$	$0.082\ ^{+0.059}_{-0.030}$
E-691 (10)	$0.22 \pm 0.03 \pm 0.02$		
NA-14 (11)	$0.18 \pm 0.03 \pm 0.03$		
Ave	0.207 ± 0.012	0.35 ± 0.06	0.098 ± 0.019

that for the spectator diagram. The fact that $\tau(\Lambda_c^+) < \tau(\Xi_c^+)$ favors the Guberina et al. model. It will be interesting to see what value of $\tau(\Omega_c^+)$ will emerge over the next year or two.

III. ABSOLUTE BRANCHING FRACTIONS

A topic of continuing importance is the scale of absolute branching fractions for the D mesons. Since the initial discovery of D meson decays, the benchmark modes for normalizing the branching fractions have been $D^0 \to K^-\pi^+$ and $D^+ \to K^-\pi^+\pi^+$. Better precision for these modes are needed to improve many important measurements, such as exclusive B branching ratios or charm semileptonic branching fractions.

CLEO (12), ARGUS (13), and ALEPH (14) have recently used the HRS technique to measure the number of D^0 decays inclusively. They look at the peak in p_t^2 or $\sin^2\alpha$ of the of the slow π^+ from $D^{*+} \to \pi^+ D^0$ with respect to the thrust axis. Because the D^{*+} direction closely follows the thrust direction and the D^{*+} decays has small q-value, the typical p_t^2 of the slow pion is typically $(40\mathrm{MeV/c})^2$, which causes a characteristic peak. Because of the CsI calorimeter, CLEO has been able to apply this to $D^{*+} \to \pi^0 D^+$ as well.

Figure 4 shows the distribution of $\sin^2\alpha$ for a number of momentum bins from the CLEO $D^0 \to K^-\pi^+$ data. There is a clear peak at low angle, corresponding to a tagged sample of 165,000 events, with a S/B as high as 2. One can determine the inclusive D^0 rate quite precisely. By measuring the fraction of these events in which a $D^0 \to K^-\pi^+$ decay is seen, one measures the absolute branching fraction. The results on absolute branching fractions are summarized in table 3. The $D^0 \to K^-\pi^+$ branching ratio is measured to 4% precision, whereas the best single earlier experiment had a 13% error. The CLEO measurement of $B(D^+ \to K^-\pi^+\pi^+)$ is much less precise, because of lower efficiency for the neutral slow pion and larger combinatoric background for the three-body decay.

IV. HADRONIC DECAYS

Although the simple picture of quark diagrams and fragmentation works well in explaining exclusive hadronic decays and therefore lifetimes, we know

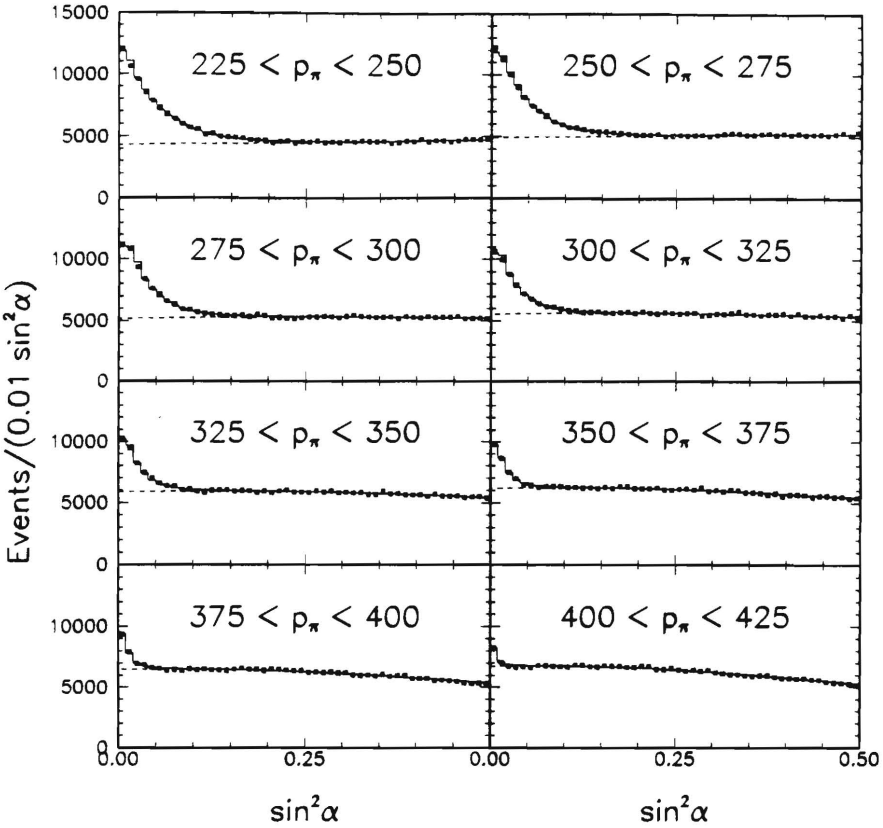

FIG. 4. Plots of $\sin^2\alpha$ for low momentum pions from CLEO data. The momentum region for each plot is shown.

TABLE 3. Absolute $B(D^0 \to K^-\pi^+)$ (%)

Exp.	$B(D^0 \to K^-\pi^+)$ (%)	$B(D^+ \to K^-\pi^+\pi^+)$ (%)
CLEO II (12)	$3.91 \pm 0.08 \pm 0.17$	$10.0 \pm 1.0 \pm 1.2$
ARGUS (13)	$4.33 \pm 0.15 \pm 0.40$	
ALEPH (14)	$3.89 \pm 0.29 \pm 0.16$	
Mark III (15)	$4.2 \pm 0.4 \pm 0.4$	$9.1 \pm 1.3 \pm 0.4$
HRS (16)	$4.5 \pm 0.8 \pm 0.5$	
Ave	3.99 ± 0.15	9.5 ± 1.0

that the success in predicting individual hadronic decays is limited. To understand why this is, it is instructive to compare D decays with K and B decays.

For K decays we use the language of isospin to describe the relative rates for exclusive final states. The important ratios are $\Gamma(K_s^0 \to \pi^0\pi^0)/\Gamma(K_s^0 \to \pi^+\pi^-) = 1/2$ and $\Gamma(K^+ \to \pi^+\pi^0)/\Gamma(K_s^0 \to \pi^+\pi^-) \approx 1/500$. We explain these two results very simply with isospin amplitudes, $A_2 << A_0$, where A_I is the amplitude to produce a state with isospin I. This is known as the $\Delta I = 1/2$ rule.

For B decays, the picture of spectator decays and factorization decribe the exclusive rates very well. The ratios of rates are $\frac{\Gamma(\overline{B}^0 \to D^0\pi^0)}{\Gamma(B^0 \to D^+\pi^-)} < 0.1$ and $\frac{\Gamma(B^- \to D^0\pi^-)}{\Gamma(B^0 \to D^+\pi^-)} \approx 2$. These results can be explained simply by the statement that $a_2/a_1 \approx 0.2$, since the $D^0\pi^0$ amplitude is proportional to a_1. On the other hand, it is not natural to use isospin amplitudes to describe this effect, since it requires accidental cancellation of two amplitudes that are comparable in size. The quark diagram picture works so well because the decay rates are not changed much by nonperturbative strong interactions and final state interactions (fsi).

The situation for D mesons is intermediate, not surprisingly. The rates $\Gamma(D^0 \to K^-\pi^+)/\Gamma(D^0 \to \overline{K}^0\pi^0)/\Gamma(D^+ \to \overline{K}^0\pi^+)$ are in the ratio 1/0.6/0.3. Neither of the isospin amplitudes is very small, as is the case for K decays. Nor is the decay rate for the a_2 mode $\Gamma(D^0 \to \overline{K}^0\pi^0)$ is small, as it is for B decay. In fact, if we used the quark diagrams and factorization, we would get the prediction $\Gamma(D^0 \to \overline{K}^0\pi^0)/\Gamma(D^0 \to K^-\pi^+) = 0.1$, while the experimental result is 0.58 ± 0.14.

Why does factorization not work as well for D decays as it does for B decays? One important reason is that substantial final state scattering of the I = 1/2 and I = 3/2 amplitudes depletes the $K^-\pi^+$ mode and enhances the $\overline{K^0}\pi^0$ mode, to the point where they are almost equal. This can be seen by writing by relating the amplitudes to the isospin amplitudes:

$$A(D^0 \to K^-\pi^+) = \sqrt{1/3}A_{3/2} + \sqrt{2/3}A_{1/2}$$
$$A(D^0 \to \overline{K}^0\ \pi^0\ ) = \sqrt{2/3}A_{3/2} - \sqrt{1/3}A_{1/2}$$
$$A(D^+ \to \overline{K}^0\pi^+) = \sqrt{3}\ A_{3/2} \qquad [\delta_{3/2} = arg(A_{3/2}),\ \delta_{1/2} = arg(A_{1/2})]$$

Mark III made the measurements some time ago, and found $|A_{3/2}/A_{1/2}| = 0.27 \pm 0.02$ and $\cos(\delta_{3/2} - \delta_{1/2}) = 0.22 \pm 0.18$. The relative phase angle is almost 90°, implying that the final state interaction is large, which is different from B decays.

To find out the values of a_1 and a_2 for these decays, one cannot directly relate them to the measured branching ratios. Instead, one needs to use the decay rates with the final state interactions taken out. This is done using the prescription $A_{K^-\pi^+} = \sqrt{1/3}|A_{3/2}| + \sqrt{2/3}|A_{1/2}|$, adding the isospin amplitudes assuming no phase angle between them. This gives the result $\Gamma(D^0 \to K^-\pi^+)_{no\ fsi} = (1.3 \pm 0.1) \times \Gamma(D^0 \to K^-\pi^+)$. It is the *no fsi* decay

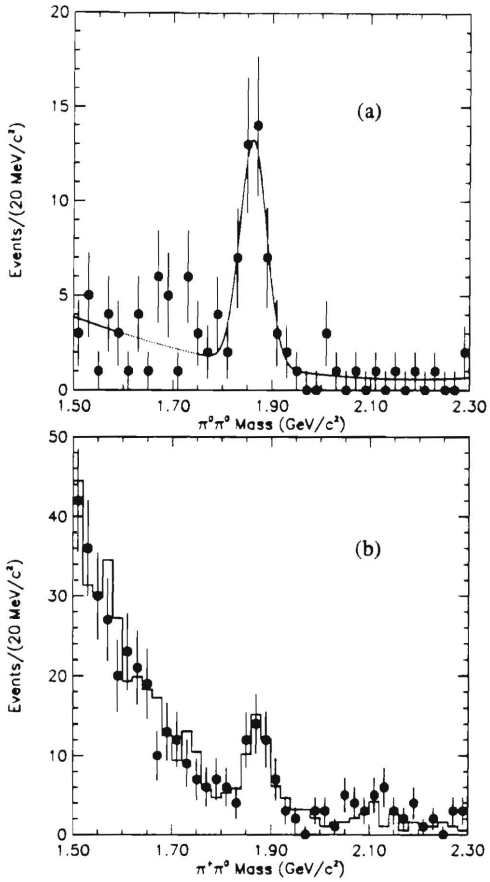

FIG. 5. CLEO signals for (a) $D^0 \to \pi^0\pi^0$ and (b)$D^+ \to \pi^+\pi^0$

rate which should be compared to the semileptonic rate in testing factorization, for example.

The first Cabibbo-suppressed charm decays observed were $D^0 \to \pi^+\pi^-$ and $D^0 \to K^+K^-$. It surprised people that the ratio $B(D^0 \to \pi^+\pi^-)/$ $B(D^0 \to K^+K^-)$ was much less than 1. One needs to take into account, however, differences in decay constants and form factors. One also needs to correct for the final state interactions, which are likely to be very different. The CLEO-II detector, with its CsI calorimeter, has made it possible to measure the two other $D \to \pi\ \pi$ decay modes needed to do this (17). The mass plots are shown in Figure 5.

The results are shown in table 4. The clearest way to interpret the results is to do an isospin decomposition of the amplitudes, analogous to the one done for $D \to K\ \pi^+$. The equations are:

TABLE 4. CLEO branching ratios for $D \to \pi\ \pi$

mode	Number	Branching ratio (%)
$D^0 \to \pi^+\pi^-$	227 ± 20	$0.127 \pm 0.011 \pm 0.011$
$D^0 \to \pi^0\ \pi^0$	40.3 ± 7.6	$0.082 \pm 0.015 \pm 0.014$
$D^+ \to \pi^+\pi^0$	34.4 ± 7.2	$0.22\ \pm 0.05\ \pm 0.05$

$$A(D^0 \to \pi^+\pi^-) = \sqrt{1/3}A_2 + \sqrt{2/3}A_0$$
$$A(D^0 \to \pi^0\ \pi^0\ ) = \sqrt{2/3}A_2 - \sqrt{1/3}A_0$$
$$A(D^+ \to \pi^+\pi^0\ ) = \sqrt{3/2}A_2 \qquad [\delta_2 = arg(A_2),\ \delta_0 = arg(A_0)]$$

And the results of the fit to the data are $|A_2/A_0| = 0.72 \pm 0.13 \pm 0.11$ and $\cos(\delta_2 - \delta_0) = 0.14 \pm 0.13 \pm 0.09$. As in the case of $D^0 \to K^-\pi^+$, the final state interactions are large, with a relative phase angle of almost 90°.

To make a sensible comparison of the branching ratio with what is expected, one needs to take out the final state interaction. If we do this, we find that $B(D^0 \to \pi^+\pi^-)_{no\ fsi} \approx B(D^0 \to \pi^+\pi^-) + B(D^0 \to \pi^0\ \pi^0\ ) \approx 1.6\ B(D^0 \to \pi^+\pi^-)$. Thus one can calculate $\left[\frac{B(D^0\to\pi^+\pi^-)}{B(D^0\to K^-\pi^+)}\right]_{no\ fsi} = 0.045 \pm 0.005$. The expected value for this ratio, taking into account different phase space and form factors, is close to 0.05. It would be interesting to carry out the same analysis with $D \to K\overline{K}$ decays, and see if the branching ratio is still higher than expected, which is a possible sign of penguin decay.

Exclusive charm decays with $\Delta C = -\Delta S$, such as $D^0 \to K^+\pi^-$ are both rare and interesting. There are two separate mechanisms that can lead to such decays: (a)mixing, in which $D^0 \to \overline{D}^0 \to K^+\pi^-$; and (b)doubly Cabibbo suppressed decays (DCSD), in which $D^0 \to K^+\pi^-$ directly. In the Standard Model, D^0 mixing is expected to be very small. One expects r_m, the ratio of mixed to unmixed decays, to be in the range $10^{-5} - 10^{-4}$, or a little larger. The corresponding parameter for DCSD is $r_{DC} = B(D^0 \to K^+\pi^-)/B(D^0 \to K^-\pi^+)$, assuming no mixing. One expects $r_{DC} = \tan^4\theta_c = 0.0026$, but variations of a factor of 2 or more are possible.

All experiments use the process $D^{*+} \to \pi^+D^0$ to tag the flavor of the D at production. One way to separate mixing and DCSD is the different time dependence. The DCSD events follow the usual $e^{-t/\tau}$ evolution, while the rate for mixed events is proportional to $t^2e^{-t/\tau}$ in the limit of small mixing. The fixed target experiments cut out events with small lifetime to reduce backgrounds, keeping full sensitivity for mixed events. The best limit is $r_m < 0.0037$ from E-691 (19), although E-687 should reach better sensitivity when they finish analyzing the full data set.

CLEO does not use information on the decay time, and is sensitive to the sum of mixing and DCSD. They observe the process $D^{*+} \to \pi^+D^0, D^0 \to K^+\pi^-$ (18). Events consistent with the Cabibbo-allowed or singly suppressed decays are explicitly vetoed. The remaining signal is 19 ± 6 events, compared to 2465 $D^0 \to K^-\pi^+$ events. The result is $r_{DC} = (0.77 \pm 0.25 \pm 0.25)\% \approx$

3 $\tan^4(\theta_C)$. Since this is significantly larger than the mixing limit, it must be predominantly due to DCSD. Knowing this number will make the analysis of mixing searches in the fixed target experiments somewhat easier.

V. SEMILEPTONIC D DECAYS

The semileptonic decays play a special role in the decays of heavy quarks. There is only one diagram, and no final state interactions, so the decays are the easiest to interpret. The diagram is shown in Fig 1(a). The momentum transfer variable is $q^2 = M^2(\ell\nu)$. The weak interaction causes a factor of $G_F V_{cs}$ in the amplitude. The strong interaction is completely described by the form factors. For the $D \to K$ transition there is a single vector form factor $f_+(q^2)$; for $D \to K^*$ there are three form factors, $A_1(q^2)$, $V(q^2)$, and $A_2(q^2)$ The Cabibbo-allowed decays of the D^0 and D^+ are related by isospin, $\Gamma(D^0 \to K^-\ell^+\nu) = \Gamma(D^+ \to \overline{K}^0\ell^+\nu)$ and $\Gamma(D^0 \to K^{*-}\ell^+\nu) = \Gamma(D^+ \to \overline{K}^{*0}\ell^+\nu)$.

We learn very different types of information from the various exclusive semileptonic decays of heavy quarks. In $c \to s$ decays, the CKM matrix element is known, and we want to measure the form factors, and check against theoretical calculations. In $b \to c$ decays, the form factors are fairly well known, and we use them to measure V_{cb}. In $b \to u$ decays, we would like to measure V_{ub}, but are hampered by the fact that the form factors for the decay to a light quark are not predicted well by models or heavy quark effective theory (HQET). We would like to measure the form factors for $D \to K(K^*)\ell\nu$ very well, and relate them to those for $B \to \pi(\rho)\ell\nu$ at high q^2. This might be done through HQET (20), lattice gauge calculations, or quark sum rules.

The largest and best measured semileptonic decay is $D \to K\ell\nu$. Table 5 shows the summary of a series of experiments which measure $R_0 = \frac{B(D^0 \to K^-\ell^+\nu)}{B(D^0 \to K^-\pi^+)}$. The largest sample is the recent measurement by CLEO (21). Figure 6 shows the results of the CLEO analysis, which made use of the decay process $D^{*+} \to \pi^+ D^0, D^0 \to K^-\ell^+\nu$. The mass difference $\delta m = m(K\ell\pi) - m(K\ell)$ shows the characteristic peak near the pion mass that is seen for hadronic decays, although it is somewhat broadened because of the missing neutrino. The $D^0 \to K^-\ell^+\nu$ sample includes 2510 events, corresponding to a measurement of $B(D^0 \to K^-\ell^+\nu)$ with 3% statistical and 5% systematic error.

If we combine the average value of R_0 from table 5 and the average $B(D^0 \to K^-\pi^+)$ from table 3, we get the results $B(D^0 \to K^-e^+\nu) = (3.71 \pm 0.20)\%$. This agrees well with results using other normalization techniques, with their larger error.

The goal of measuring the decay $D^0 \to K^-\ell^+\nu$ is to determine the form factor $f_+(q^2)$, which represents the amplitude that the $(s\bar{q})$ state forms a K meson. The energy of the K in the D rest frame, E_K, is linearly related to q^2, $q^2 = (M_D^2 + q^2 - M_K^2)/2\,M_D$. At $q^2 = q^2_{max} = (M_D - M_K)^2$, the K is at rest in the D frame ($E_K = M_K$). The overlap of the initial and final state

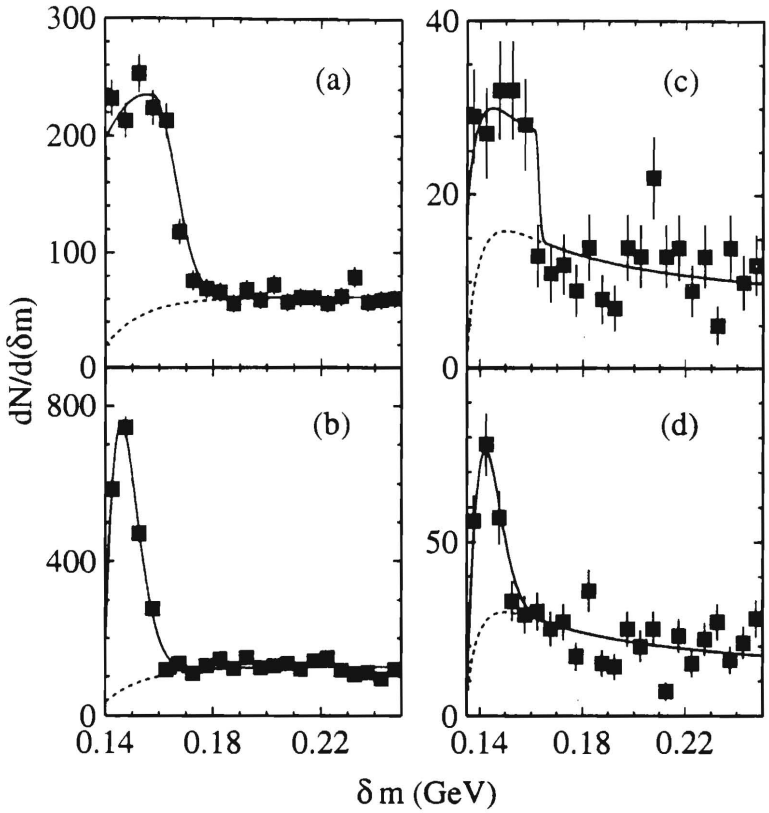

FIG. 6. Signals for $D \to \overline{K}\ell^+\nu$ from CLEO. The process observed is $D^* \to \pi + D, D \to K\ell\nu$, and $\delta m = m_{K\ell\pi} - m_{K\ell}$. The plots are for D^0 , $m_{K\ell}$= 1.2-1.4 GeV (a) and 1.4-1.8 GeV (b); and $D^+, m_{K\ell}$= 1.2-1.4 GeV (c) and 1.4-1.8 GeV (d).

TABLE 5. Measurements of $R_0 = \frac{B(D^0 \to K^-\ell^+\nu)}{B(D^0 \to K^-\pi^+)}$ (The branching ratios for muon samples are corrected to electron equivalents.)

Exp	Lepton	Events	$\frac{B(K^-\ell^+\nu)}{B(K^-\pi^+)}$
CLEO II (21)	e, μ	2510	$0.978 \pm 0.027 \pm 0.044$
E-687 (22)	μ	340	$0.82 \pm 0.13 \pm 0.13$
E-691 (23)	e	250	$0.90 \pm 0.07 \pm 0.11$
CLEO 1.5 (24)	e	584	$0.91 \pm 0.06 \pm 0.06$
CLEO 1.5 (24)	μ	231	$0.79 \pm 0.08 \pm 0.09$
Ave			0.931 ± 0.038

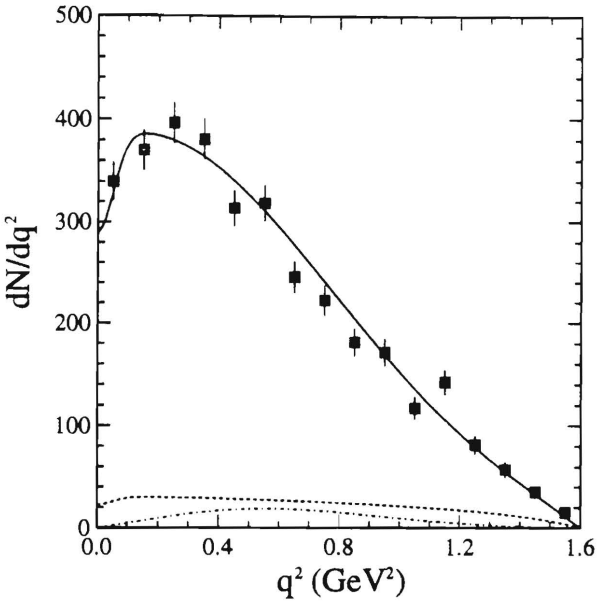

FIG. 7. The fit to the q^2 distribution for the CLEO $D^0 \to K^-\ell^+\nu$ sample

wave functions is as large as possible and the form factor is at its maximum. At $q^2 = 0$, $E_K = (M_D^2 + M_K^2)/(2\ M_D) \approx 1.0$ GeV, and the form factor is at its minimum.

The differential decay rate for $D \to K\ell\nu$ has a simple dependence on the single vector form factor:

$$\frac{d\Gamma}{dq^2} = \frac{G^2}{24\pi^3}\ |V_{cs}|^2\ P_K^3\ f_+^2(q^2). \tag{1}$$

From the branching fraction and the lifetimes already quoted, one can calculate the decay rate, $\Gamma(D^0 \to K^-\ell^+\nu) = (9.0 \pm 0.5) \times 10^{10} s^{-1}$. This determines the normalization of the form factor: $f_+(0) = 0.77 \pm 0.04$. I will compare this with theoretical predictions below.

The shape of the form factor is a measure of the decreasing overlap of the D and K wave functions as E_K increases. CLEO has measured this shape with the large $D^0 \to K^-\ell^+\nu$ sample. The dominant q^2 dependence is from the P_K^3 term in equation (1), which causes the differential decay rate to peak at low q^2. The factor $f_+^2(q^2)$ increases with q^2, changing by a factor of about 2 over the kinematic range of the decay.

Figure 7 shows the measured q^2 spectrum for the $D \to \overline{K}\ell^+\nu$ candidates. A good fit to the data is obtained with either of two forms used in theoretical models. The first form is $f_+(q^2) = f_+(0)e^{\alpha q^2}$, which is used in ISGW. The result of the fit is $\alpha = (0.29 \pm 0.04 \pm 0.06)\ \mathrm{GeV}^{-2}$, which agrees with the value of 0.21 chosen by ISGW. The second form is $f_+(q^2) = f_+(0)/(1 - q^2/M^{*2})$.

TABLE 6. Measurements of $\Gamma(D \to K^*\ell^+\nu)$. The normalization values used were $\Gamma(D^0 \to K^-\pi^+) = (9.3 \pm 0.4) \times 10^{10}s^{-1}$ (CLEO II); $\Gamma(D^0 \to K^-\ell^+\nu) = (9.0 \pm 0.5) \times 10^{10}s^{-1}$ (CLEO 1.5); and $\Gamma(D^+ \to K^-\pi^+\pi^+) = (9.0 \pm 1.0) \times 10^{10}s^{-1}$ (others).

Exp	$K^*\ell\nu$ mode	normalization	$\Gamma(D \to K^*\ell^+\nu)$ $(10^{10}s^{-1})$
CLEO-II (21)	Both	$K^-\pi^+$	5.7 ± 0.7
E-687 (25)	D^+	$K^-\pi^+\pi^+$	5.0 ± 0.9
E-691 (26)	D^+	$K^-\pi^+\pi^+$	4.4 ± 0.8
E-653 (27)	D^+	$K^-\pi^+\pi^+$	4.2 ± 1.2
ARGUS (28)	D^+	$K^-\pi^+\pi^+$	5.0 ± 1.3
CLEO 1.5 (24)	D^0	$K^-\ell^+\nu$	4.6 ± 1.7
Ave			5.1 ± 0.5

For this fit, the result is $M^* = (2.00 \pm 0.11 \pm 0.16)\ GeV$, which is in good agreement with the value of 2.1 GeV expected from the closest resonance with the proper quantum numbers, the D_s^*. The measured value of M^* agrees with earlier experiments but with significantly better error. Either form gives a good parameterization of the form factor.

There have been a number of measurements of $B(D \to K^*\ell^+\nu)$, with both D^0 and D^+ mesons. Table 6 shows measurements of the decay rate $\Gamma(D \to K^*\ell^+\nu)$. I have used for each experiment the branching ratio relative to the normalization mode listed, and the average from this review for the normalization mode. The average value from these measurements is $\Gamma(D \to K^*\ell^+\nu) = (5.1 \pm 0.5) \times 10^{10}s^{-1}$, which is substantially lower than the early predictions.

To understand the low value of $\Gamma(D \to K^*\ell^+\nu)/\Gamma(D \to \overline{K}\ell^+\nu)$, one must look at the form factors directly. The amplitude for semileptonic decay to a vector meson has three form factors.(recall $q^2 = M^2_{\ell\nu}$)

$A = \frac{G_F}{\sqrt{2}} V_{cs} L^\mu H_\mu$.

$$
\begin{aligned}
H_\mu = & A_1(q^2)\ \ \varepsilon_\mu(M_D + M_{K^*}) && s-wave \\
& - V\ (q^2)\ \ 2i\epsilon_{\mu\nu\rho\sigma}\varepsilon^\nu P^\rho K^\sigma/(M_D + M_{K^*}) && p-wave \\
& - A_2(q^2)\ \ (\varepsilon_\nu P^\nu)(P+K)_\mu/(M_D + M_{K^*}) && d-wave
\end{aligned}
$$

Here P^μ is the D momentum, and $\varepsilon^\mu(K^\mu)$ is the K* polarization(momentum). The rate is dominated by the A_1 form factor. The ratios of form factors are determined by fitting the angular distributions. In the fits made to date, it has been assumed that the q^2 dependence of the form factors follows that of the $K\ell\nu$ form factor. As the precision of the measurements improve, the correctness of this assumption will have to tested.

With all of these measurements, we have accurate measurements of two form factors, f_+ and A_1, and coarser measurements of V and A_2. The goal is to compare a complete set of these form factor measurements with the various calculations, either using quark models, lattice gauge calculations, or quark sum rules. This is done in table 8. The ratios of form factors, which may be more reliably predicted, can also be compared using this table.

TABLE 7. Form Factor Ratios in $D \to K^* \ell^+ \nu$

Exp.	$R_v = V/A_1$	$R_2 = A_2/A_1$
E-687 (25)	$1.74 \pm 0.27 \pm 0.28$	$0.78 \pm 0.18 \pm 0.10$
E-653 (29)	$2.00 \pm 0.33 \pm 0.16$	$0.82 \pm 0.22 \pm 0.11$
E-691 (26)	$2.0 \pm 0.6 \pm 0.3$	$0.0 \pm 0.5 \pm 0.2$
Ave	1.90 ± 0.25	0.74 ± 0.15

TABLE 8. Form Factors: Comparison with Theory

Source		$f_+(0)$	$A_1(0)$	$V(0)$	$A_2(0)$
Exp	Ave	0.77 ± 0.04	0.61 ± 0.05	1.16 ± 0.16	0.45 ± 0.09
Quark	ISGW (30)	0.8	0.8	1.1	0.8
Models	WSB (31)	0.76	0.88	1.3	1.2
	KS (32)	0.7	0.82	0.8	0.8
	AW/GS (33)	0.7	0.8	1.5	0.6
Lattice	BKS (34)	0.76	0.83	1.4	0.6
Gauge	LMMS (35)	0.63	0.53	0.9	0.2
Sum Rules	BBD (36)	0.60	0.5	1.1	0.6

Looking at table 8, certain conclusions can be reached. For f_+, most calculations agree with data, although the LMMS and BBD versions are somewhat low. The calculations of A_1 are mostly high by a factor of 1.4 or so, which corresponds to about a factor of two in rate. The exceptions are LMMS and BBD, which agree rather well. For V, almost all of the calculations agree within the present large errors. Finally, the quark model estimates of A_2 are generally high, although the other methods agree within large experimental and theoretical errors.

The Cabibbo-supressed decay $D \to \pi \ell \nu$ has also been observed. Since the ratio $|V_{cd}/V_{cs}|$ is known from unitarity, the measurement of $\Gamma(D \to \pi \ell \nu)/\Gamma(D \to K \ell \nu)$ serves to determine f_+^π/f_+^K, which is predicted to be in the broad range 0.7–1.4. Mark III saw 7 events of the type $D^0 \to \pi^- \ell^+ \nu$, giving a branching ratio of $(0.39^{+0.24}_{-0.11} \pm 0.04)\%$ (37). This corresponds to $f_+^\pi/f_+^K = 1.0^{+0.6}_{-0.3} \pm 0.1$. In a recent analysis, CLEO observed 53 ± 8 examples of $D^{*+} \to \pi^0 D^+, D^+ \to \pi^0 \ell^+ \nu$, corresponding to $B(D^+ \to \pi^0 \ell^+ \nu)/B(D^+ \to \overline{K}^0 \ell^+ \nu) = (8.5 \pm 2.7 \pm 1.4)\%$ (38). Keeping in mind that the $\Gamma(D^+ \to \pi^0 \ell^+ \nu)/\Gamma(D^0 \to \pi^- \ell^+ \nu) = 1/2$ (not 1), this result yields $f_+^\pi/f_+^K = 1.29 \pm 0.21 \pm 0.11$. This is somewhat high, but one would like to have better statistical precision on this measurement before drawing a conclusion about the relative form factors.

With all of this experimental information on semileptonic D decays, we can inquire whether the pseudoscalar and vector mesons dominate the inclusive semileptonic rates. Table 9 summarizes the experimental information. The inclusive decay rate is measured by Mark III to be $(17.0 \pm 1.4) \times 10^{10} s^{-1}$ (39). Thus the modes not included here contribute only $(8 \pm 11)\%$ of the inclusive

TABLE 9. Summary of D Semileptonic Rates

Mode	Source	$\Gamma(10^{10}s^{-1})$
$D \to \overline{K}\ell^+\nu$	D^0	9.0 ± 0.5
$D \to K^*\ell^+\nu$	$D^0 + D^+$	5.1 ± 0.5
$D \to \pi\ \ell\ \nu$	$D^0 + D^+$	1.2 ± 0.3
$D \to \rho\ \ell\ \nu$	theory	0.3 ± 0.1
Total		15.6 ± 0.8

TABLE 10. Measurements of $R_s = \frac{B(D_s^+ \to \phi\ \ell^+\nu)}{B(D_s^+ \to \phi\ \pi^+)}$

Exp	Events	R_S
E-687 (41)	97	$0.58 \pm 0.17 \pm 0.07$
CLEO (42)	54	$0.49 \pm 0.10\ ^{+0.10}_{-0.14}$
ARGUS (43)	104	$0.57 \pm 0.15 \pm 0.15$
Ave		0.54 ± 0.10

rate. This agrees with tight limits from explicit searches for higher modes such as $D \to K^*\pi\ell\nu$. (40) The interpretation of this result is that the final state s quark from charm semileptonic decay is usually produced with a small enough momentum that it is bound in an $l = 0$ $q\bar{q}$ meson.

The measurements of D_s^+ semileptonic decays are not as advanced as those for the D mesons, of course. The decay $D_s^+ \to \phi\ \ell^+\nu$ is the easiest to observe, and has been seen in a number of experiments. By measuring the ratio $R_s = B(D_s^+ \to \phi\ \ell^+\nu)/B(D_s^+ \to \phi\ \pi^+)$, and combining it with theoretical estimates of $\Gamma(D_s^+ \to \phi\ \ell^+\nu)/\Gamma(D \to K^*\ell^+\nu)$ and measurements of $\Gamma(D \to K^*\ell^+\nu)$ and $\tau(D_s^+)$, it is possible to determine the absolute branching fraction for the benchmark mode, $B(D_s^+ \to \phi\ \pi^+)$. The measurements of R_s are summarized in table 10. Using the average value, one gets $B(D_s^+ \to \phi\ \pi^+) = (3.6 \pm 0.6 \pm 0.4)\%$. This number is useful for a wide range of B and charm physics.

The weak point of determining the absolute branching fraction this way is the theoretical estimate of the ratio of D_s^+ and D^+ decay rates. Form factor models predict very similar values for the two decays. On the other hand, E-653 finds for the one ratio of form factors $R_2 = 2.1^{+0.6}_{-0.5} \pm 0.2$ (44), compared to the lower values for the D^+ decay shown in table 7. This number is based on a multidimensional fit to the angular distribution for 19 events. It is worth waiting until similar analyses are done with larger data samples, which should be very soon.

The semileptonic decays of the D_s^+ to pseudoscalar mesons are shared between the η and η'. These modes are particularly interesting because CLEO has measured surprisingly large branching ratios for the related hadronic modes: $B(D_s^+ \to \eta\ \rho^+)/B(D_s^+ \to \phi\ \pi^+) = 2.86 \pm 0.38 \pm 0.37$ compared to a BSW prediction of 1.96, and $B(D_s^+ \to \eta'\rho^+)/B(D_s^+ \to \phi\ \pi^+) = 3.44 \pm 0.62 \pm 0.45$, compared to 0.56 (45). Thus the sum of these two modes

is about 2.5 times the expected value, and it is hard to see how this can come about from final state interactions. One could imagine such an enhancement if W-annihilation decays were significant.

E-653 has measured $B(D_s^+ \to (\eta + \eta')\mu^+\nu)/B(D_s^+ \to \phi\ \mu^+\nu) = 3.9 \pm 1.6$ (44). This is about twice as large as in semileptonic D decays. On the other hand, Kamal*et al.* (46) have shown that it agrees well with what one would infer from the large hadronic modes, using factorization. The errors are still very large, however, and again we will need more data to see if the D_s^+ semileptonic decays mirror the D decays.

VI. SEMILEPTONIC Λ_C DECAYS

The semileptonic decays of baryons with heavy quarks provide an interesting opportunity to test many of the predictions of HQET. The experimental information is not yet as detailed as that available for D decay, however. The decay diagram is similar to the hadronic decay diagram shown in figure 2(a). The final state strange baryon must have isospin 0, so should be either a Λ or Λ^*. If the final state hadron has $l = 0$, as it does for D decays, then $J^P = 1/2^+$. Thus the decay $\Lambda_c \to \Lambda\ \ell^+\nu$ decay should dominate, in the same way that $K + K^*$ does for D decays. The inclusive semileptonic decay rate should be approximately the same as it is for D decays. This and the Λ_c lifetime lead to the prediction $B(\Lambda_c \to \ell^+) = (3.4 \pm 0.4)\%$.

ARGUS and CLEO observe the decay $\Lambda_c \to \Lambda X \ell^+\nu$, where the X represents possible other hadrons (47,48). The $M(\Lambda\ell)$ mass spectrum for the CLEO sample is shown if figure 8. There is an excess of $530 \pm 27 \pm 40$ events in the right sign data with $M(\Lambda\ell) < M(\Lambda_c)$. CLEO has also shown that less than 15% of this has accompanying hadrons, so it is predominantly the decay $\Lambda_c \to \Lambda\ell^+\nu$, as expected. The cross section times branching ratio for this process is measured to be $\sigma B(\Lambda_c \to \Lambda X \ell^+\nu) = (5.23 \pm 0.27 \pm 0.83)$ pb (CLEO) and $(4.15 \pm 1.03 \pm 1.18)$ pb (ARGUS).

We can use the estimate made above of the inclusive semileptonic branching fraction and this measurement to set a scale for the Λ_c absolute branching fraction scale, which is set by $B(\Lambda_c \to pK^-\pi^+)$. The measurements to use are $B(\Lambda_c \to pK^-\pi^+)/B(\Lambda_c \to \Lambda X \ell^+\nu) = 1.9 \pm 0.1 \pm 0.3$ (CLEO) and $2.7 \pm 0.8 \pm 0.6$ (ARGUS). Assuming that the fraction of the inclusive rate that goes into this mode is 0.8 ± 0.2, using the inclusive semileptonic branching fraction estimated above, and taking the average of CLEO and ARGUS measurements, one gets for the absolute branching fraction $B(\Lambda_c \to pK^-\pi^+) = (4.9 \pm 1.7)\%$. This agrees with measurements using other techniques in this energy range (49,50), but is a factor of two greater than an older measurement by Mark II (51).

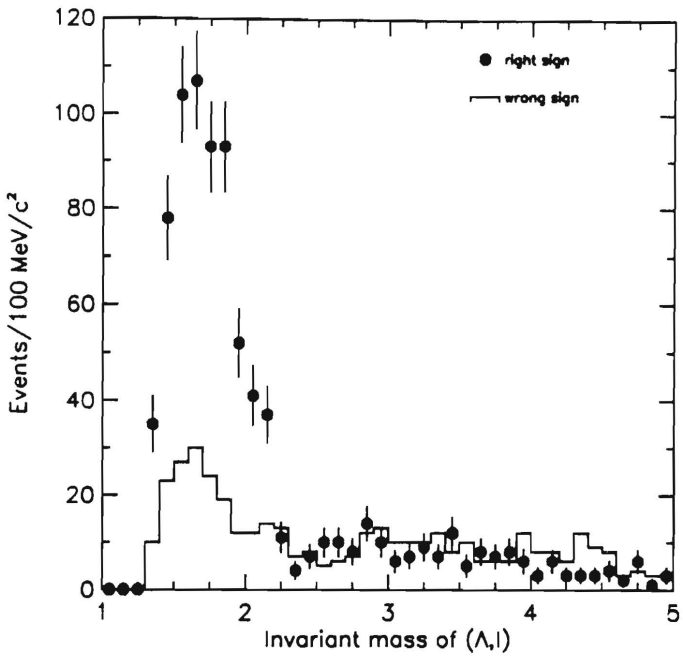

FIG. 8. The $M(\Lambda\ell)$ mass spectrum for the CLEO sample of $\Lambda_c \to \Lambda X \ell^+ \nu$.

VII. LEPTONIC DECAYS AND DECAY CONSTANTS

The decay constants of the heavy pseudoscalar mesons (f_D, f_B) are of great interest for the study of mixing and CP violation. The rate for B mixing is proportional to f_B^2, so the measurement of V_{td} from mixing is proportional to $1/f_B$. For the leptonic decay of a pseudoscalar meson P, described by the diagram in fig. 1(d), the decay rate is

$$\Gamma(P(Q\overline{q}) \to \ell\overline{\nu_\ell}) = \frac{G_F^2}{8\pi}|V_{Qq}|^2 f_P^2\ m_P\ m_\ell^2[1 - m_\ell^2/m_P^2]^2 \qquad (2)$$

The estimated rate for $B(B^+ \to \tau^+\nu) \approx 10^{-4}$, so it will not be measured soon. The theoretically expected range for f_B is from 140–270 MeV, which corresponds to a factor of 4 uncertainty in the decay or mixing rate. The best hope we have of narrowing this range with experimental data is to measure the charm decay constant. Then, using lattice gauge calculations or other techniqes, one can extrapolate to f_B. Naive scaling based on a simple picture of heavy meson wave functions predicts $f_B/f_D = \sqrt{m_d/m_b} = 0.6$. The lattice gauge caluculations find substantial corrections to this, getting values for this ratio in the range 0.8–0.9 (53,52).

The value of f_D is expected to be in the range 170–300 MeV, with f_{D_S} about 10% larger. With values in this range, the branching ratios are expected to be

$B(D^+ \to \mu^+\nu) = (2-7) \times 10^{-4}$ and $B(D_S^+ \to \mu^+\nu) = (3-9) \times 10^{-3}$. Mark III has placed an upper limit on the D^+ decay, $B(D^+ \to \mu^+\nu) < 7.2 \times 10^{-4}$, corresponding to a limit on the decay constant $f_D < 290$ MeV (54). There is new information on the D_S^+ decay from two emulsion experiments and from CLEO.

The emulsion experiments are able to measure the D^+ direction with some accuracy before it decays. They use this to measure $p_{T\mu}$, the transverse momentum of the muon relative to the D^+ direction. The maximum value of muons from semileptonic decays is about 0.88 GeV/c, while the leptonic decays from the $D_S^+(D^+)$ give a Jacobian peak at 0.98(0.93) GeV/c. If the fake muons are small, the pure leptonic decay events should be visible beyond the endpoint in the $p_{T\mu}$ spectrum.

WA-75 has observed 6 events with $p_{T\mu} > 0.90$ GeV/c, with an estimated background, including from D^+ leptonic decays, of 0.8 (55). Turning this into a branching ratio is somewhat difficult, since they observe no other D_s^+ modes cleanly. They measure the yield relative to inclusive semileptonic D^0 decays, with the result $\sigma B(D_s^+ \to \mu^+\nu)/\sigma B(D^0 \to X\,\mu^+\nu) = (1.25^{+0.55+0.24}_{-0.44-0.20}) \times 10^{-2}$. Using measurments of the D^0 and D_s^+ cross sections from NA-32 and the inclusive semileptonic branching ratio from Mark III, they calculate $B(D_s^+ \to \mu^+\nu) = (4.0^{+1.8+0.8}_{-1.0-0.6} \pm 1.7) \times 10^{-3}$, corresponding to $f_{D_S} = (232 \pm 45 \pm 20 \pm 48)$ MeV. The third error is the systematic error on the normalization.

E-653 is doing a similar analysis with a larger data sample (56). Figure 9 shows the $p_{T\mu}$ spectrum from an analysis of 1/3 of their data. There is an excess of events beyond the endpoint of the expected semileptonic spectrum. A fit yields a total of 23 events consistent with the decay $D_s^+ \to \mu^+\nu$. They will have about 70 events in the full sample, and will be able to normalize to the $D_S^+ \to \phi\,\mu^+\nu$ signal they see. They are not ready to quote a branching ratio now, however. There are also 3 candidates showing a kink in the short-lived track, consistent with the decay $D_S^+ \to \tau^+\nu$.

CLEO-II has used a very different approach to observe $D_s^+ \to \mu^+\nu$, in which they observe the process $D_s^{*+} \to \gamma D_s^+, D_s^+ \to \mu^+\nu$ (57). The missing momentum and energy in the hemisphere of the muon are used to estimate $\mathbf{p}_\nu$ and E_ν. For events in a broad $\mu\nu$ mass range around the D_s mass, the mass difference $\Delta M = M(\mu\nu\gamma) - M(\mu\nu)$ is plotted. Since the purely electronic decay is negligible, a similar spectrum for electrons serves as an ideal background sample. After taking into account differences in efficiencies and fake rates, they make the background-subtracted ΔM spectrum shown in fig. 10. There is a continuum from $D_s^+ \to \mu^+\nu$ combined with random gammas, and a peak at the expected mass from D_s^* decay. There are 39 ± 8 events in the peak.

CLEO measures the branching ratio for the leptonic decay relative to the benchmark $\phi\,\pi^+$ mode.The result is $\Gamma(D_s^+ \to \mu^+\nu)/\Gamma(D_s^+ \to \phi\,\pi^+) = 0.245 \pm 0.052 \pm 0.074$. They combine this with the value $B(D_s^+ \to \phi\,\pi^+) = (3.7 \pm 0.9)\%$ to measure the decay constant $f_{D_S} = 344 \pm 37 \pm 52 \pm 42$ MeV, where the last error is due to the uncertainty in the normalizing branching ratio. This result

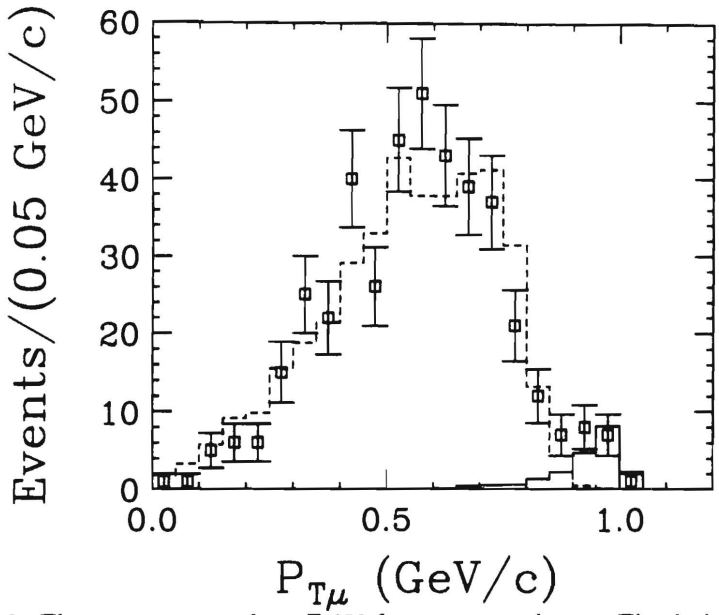

FIG. 9. The $p_{T\mu}$ spectrum from E-653 for one-prong decays. The dashed curve is the prediction for semileptonic decays, and the solid curve is the shape expected for the leptonic decay.

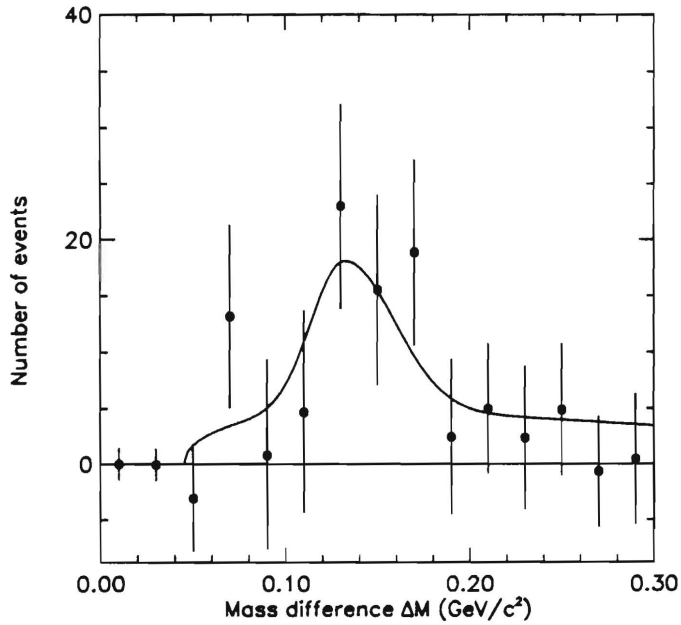

FIG. 10. The ΔM spectrum from CLEO, showing evidence of the decay $D_s^+ \to \mu^+\nu$

is at the upper end of the theoretical predictions, but it is only 1 standard deviation from the WA-75 value.

VIII. CONCLUSIONS

The pattern of charm meson lifetimes can be understood fairly well with a simple model of spectator decays. Charm baryon lifetimes show the effect of additional spectator and non-spectator decay diagram. Simple models do not reproduce the individual hadronic branching ratios, however. This is partly due to large final state interactions, which have been measured for some modes.

It is easier to interpret exclusive semileptonic decays. The form factors for the dominant D semileptonic decays are fairly well measured, although some need larger data samples. Much theoretical work is underway to understand these, and to gain what insight one can about the $b \to u$ exclusive semileptonic decays that will be needed to measure V_{ub} accurately.

The scale of absolute branching fractions has been measured very accurately for the D^0, somewhat less so for the D^+. This is important for precise measurements of a wide range of D and B decays.

Finally, there is evidence of the leptonic decay $D_s^+ \to \mu^+\nu$, and the first measurements of f_{D_S}. We can look forward to the value of the decay constant to improve over the next few years as larger data samples become available.

Our knowledge of charm decays is extensive. The leading new results are either detailed measurements of important quantities, such as semileptonic form factors, or discovieries of rare processes, such as leptonic decays. Additional improvements will come with larger data samples coming from all three types of charm experiments in the next couple years.

IX. ACKNOWLEDGMENTS

Two recent review talks on charm physics were of great help in preparing this talk: one by John Cumalat at the Fermilab DPF meeting, and one by Pat Burchat at the Montreal Heavy Flavour Symposium. I have repeatedly cornered my colleagues at Santa Barbara, Rolly Morrison, Harry Nelson, and Jeff Richman, and forced them to discuss some of the issues raised here. I am grateful to my colleagues in CLEO working on charm decay physics, as well as members of the other experiments discussed, for promptly providing the many plots, papers, and references I needed.

REFERENCES

1. G. Goldhaber it et al., Phys. Rev. Lett. **37**, 255 (1976); I. Peruzzi it et al., Phys. Rev. Lett. **37**, 569 (1976).

2. S.L. Glashow, J. Iliopoulos, and L. Maiani, Phys. Rev. D**2**, 1285 (1970).
3. M. Bauer, B. Stech, and M. Wirbel, Z. Phys. C**34**, 103 (1987).
4. P. Frabetti *et al.* (E-687), Phys. Rev. Lett. **72**, 827 (1993) for the D_s^+; for the other two lifetimes, Fermilab seminar and private communication.
5. J. Raab *et al.* (E-691), Phys. Rev. D**37**, 2391 (1988).
6. B. Guberina *et al.*, Z. Phys. C**33**, 297 (1986).
7. M.B. Voloshin and M.A. Shifman, Sov. Phys. JETP **64**, 698 (1986).
8. P. Frabetti *et al.* (E-687), Phys. Rev. Lett. **70**, 1381 (1993); **70**, 1755 (1993); **70**, 2058 (1993).
9. S. Barlag *et al.* (NA-32), Phys. Lett. B**218**, 374 (1989) **233**, 522 (1989); **236**, 495 (1990).
10. J.C. Anjos *et al.* (E-691), Phys. Rev. Lett. **60**, 1379 (1988).
11. M.P. Alvarez *et al.* (NA-14), Z. Phys. C**47**, 539 (1990).
12. D. Akerib *et al.*, CLEO preprint CLEO 93-16 (1993), submitted to Phys. Rev. Lett for the D^0; CLEO collaboration, paper submitted to this conference for the D^+.
13. ARGUS collaboration, paper submitted to this conference.
14. ALEPH collaboration, paper submitted to this conference.
15. J. Adler *et al.* (Mark III), Phys. Rev. Lett. **60**, 89 (1988).
16. S. Abachi *et al.* (HRS), Phys. Lett. B**205**, 411 (1988).
17. M. Selen *et al.* (CLEO), preprint CLEO 93-6, to appear in Phys. Rev. Lett. (1993).
18. CLEO collaboration, paper submitted to this conference.
19. J.C. Anjos *et al.* (E-691), Phys. Rev. Lett. **60**, 1239 (1988).
20. N. Isgur and M.B. Wise, Phys. Rev. D**42**, 2388 (1989).
21. A. Bean *et al.*, CLEO preprint CLEO 93-18, submitted to Phys. Lett. B. (1993).
22. P.L. Frabetti *et al.* (E-687), preprint Fermilab-Pub-93/194-E, submitted to Phys. Lett. B (1993).
23. J.C. Anjos *et al.* (E-691), Phys. Rev. Lett. **62**, 1587 (1989).
24. G. Crawford *et al.* (CLEO), Phys. Rev. D**44**, 3394 (1991).
25. P.L. Frabetti *et al.* (E-687), Phys. Lett. B**307**, 262 (1993).
26. J.C. Anjos *et al.* (E-691), Phys. Rev. Lett. **62**, 722 (1989); **65**, 2630 (1990).
27. K. Kodama *et al.* (E-653), Phys. Lett. B**286**, 187 (1992).
28. H. Albrecht *et al.* (ARGUS), Phys. Lett. B**255**, 634 (1991).
29. K. Kodama *et al.* (E-653), Phys. Lett. B**274**, 246 (1992).
30. N. Isgur *et al.*, Phys. Rev. D**39**, 799 (1989).
31. M. Wirbel *et al.*, Z. Phys. C**29**, 627 (1985).
32. J.G. Körner and G.A. Schuler, Z. Phys. C**38**, 511 (1988).
33. T. Altomari and L. Wolfenstein, Phys. Rev. C**37**, 681 (1988); F.J. Gilman and R.L. Singleton, Phys. Rev. D**41**, 142 (1990).
34. C.W.Bernard, A.X. El-Khadra, and A. Soni, Phys. Rev. D**47**, 998 (1993).
35. V. Lubicz *et al.*, Phys. Lett. B**274**, 415 (1992).
36. P. Ball, V.M. Braun, and H.G. Dosch, Phys. Rev. D**44**, 3567 (1991).
37. J. Adler *et al.* (Mark III), Phys. Rev. Lett. **62**, 1821 (1989).
38. M.S. Alam *et al.* (CLEO), Phys. Rev. Lett. **71**, 1311 (1993).
39. R. Baltrusaitis *et al.* (Mark III), Phys. Rev. Lett. **54**, 1978 (1985).
40. K. Kodama *et al.* (E-653), preprint CMU-HEP 93-14, to appear in Phys. Lett. (1993).
41. P.L. Frabetti *et al.* (E-687), preprint Fermilab-Pub-93/184-E, submitted to

Phys. Lett. B (1993).
42. J. Alexander *et al.* (CLEO), Phys. Rev. Lett. **65**, 1531 (1990).
43. H. Albrecht *et al.* (ARGUS), Phys. Lett. B**255**, 634 (1991).
44. K. Kodama *et al.* (E-653), Phys. Lett. B**309**, 483 (1993).
45. J. Alexander *et al.* (CLEO), Phys. Rev. Lett. **68**, 1275 (1992); 1279 (1992).
46. A.N. Kamal, Q.P. Xu, and A. Czarnecki, preprint Alberta-Thy-3-93, submitted to this conference.
47. H. Albrecht *et al.* (ARGUS), Phys. Lett. B**269**, 234 (1991); paper submitted to this conference.
48. F. Butler *et al.* (CLEO), paper submitted to this conference (1993).
49. P. Avery *et al.* (CLEO), Phys. Rev. D**43**, 3599 (1991).
50. H. Albrecht *et al.* (ARGUS), Phys. Lett. B**210**, 263 (1988).
51. G. Abrams *et al.* (Mark II), Phys. Rev. Lett. **44**, 10 (1980).
52. C.W. Bernard, J.N. Labrenz, and A. Soni, Washington U. preprint UW-PT-93-06, (1993). Phys. Rev. D**47**, 998 (1993).
53. A. Abada *et al.*, Nucl. Phys. B**376**, 172 (1992); G. Martinelli, talk at the Heavy Flavor Symposium, Montreal (1993).
54. J. Adler *et al.* (Mark III), Phys. Rev. Lett. **60**, 1375 (1988).
55. S. Aoki *et al.* (WA-75), Prog. Theor. Phys. **89** ,131 (1993).
56. E-653 Collaboration, paper submitted to this conference (1993).
57. Y. Kubota *et al.* (CLEO), preprint CLEO 93-14, submitted to Phys. Rev. D. (1993).